

The Majorana neutrino mass matrix indicated by the current data

Xinyi Zhang,^a Bo-Qiang Ma^{1a,b,c}

^a*School of Physics and State Key Laboratory of Nuclear Physics and Technology, Peking University, Beijing 100871, China*

^b*Collaborative Innovation Center of Quantum Matter, Beijing, China*

^c*Center for High Energy Physics, Peking University, Beijing 100871, China*

E-mail: xzhang_phy@pku.edu.cn, mabq@pku.edu.cn

ABSTRACT: The Majorana neutrino mass matrix combines information from the neutrino masses and the leptonic mixing in the flavor basis. Its invariance under some transformation matrices indicates the existence of certain residual symmetry. We offer an intuitive display of the structure of the Majorana neutrino mass matrix, using the whole set of the oscillation data. The structure is revealed in dependence on the lightest neutrino mass. We find that there are three regions with distinct characteristics of structure. A group effect and the μ - τ exchange symmetry are observed. Implications for flavor models are discussed.

¹Corresponding author.

Contents

1	Introduction	1
2	Reconstruct the Majorana neutrino mass matrix	2
2.1	input	2
2.2	extreme case	3
2.3	general case	4
3	Discussion	5
3.1	regional characteristics	5
3.2	μ - τ exchange symmetry	7
3.3	effects of the Majorana phases	8
4	Conclusion	8
A	The expressions of the entries of the Majorana neutrino mass matrix	9
B	The same procedure with Fogli et al. data	10
C	The effects of the Majorana phases in the case of inverted ordering	10

1 Introduction

Neutrino oscillation has been well established by various experiments regarding solar [1, 2], atmospheric [3–6] and reactor [7–10] neutrinos. The oscillation is caused by the mismatch of the neutrino mass eigenstates with the flavor eigenstates.

Generally, the oscillation probability measured by the oscillation experiments depends on the neutrino energy, the distance of flight, the mixing matrix elements and the squared mass differences. The physical parameters in the oscillation probability are $\theta_{12}, \theta_{23}, \theta_{13}, \delta$ coming from the Pontecorvo-Maki-Nakawaga-Sakata (PMNS) matrix [11, 12] and two squared mass differences $\Delta m_{21}^2, \Delta m_{31(2)}^2$ correspond to two observed frequencies of the oscillation probability. These parameters involve information on both mass and mixing. For Majorana neutrinos, the Lagrangian part regarding the leptonic masses and mixing is

$$\mathcal{L} = \frac{g}{\sqrt{2}} \bar{l}_L \gamma^\mu \nu_L W_\mu^+ + \bar{E}_R m_l l_L + \frac{1}{2} \bar{\nu}_L M \nu_L^c + \text{H.c.}, \quad (1.1)$$

where $l_L = (e_L, \mu_L, \tau_L)^T, \nu_L = (\nu_{eL}, \nu_{\mu L}, \nu_{\tau L})^T, E_R = (e_R, \mu_R, \tau_R)^T$. We choose the flavor basis, i.e., the charged lepton mass eigenstates coincide with the flavor eigenstates, then the information about mixing is contained solely in the Majorana mass matrix, together with the mass information.

From a theoretical viewpoint, a Majorana neutrino mass matrix stemming from a dimensional-5 Weinberg operator [13] can give a natural explanation of the smallness of the neutrino mass, as explored by various seesaw models [14–19]. Besides, the invariance of the Majorana mass matrix under some transformation matrices shows evidences for the existence of certain flavor symmetry, and extensive works are dedicated on this issue (see [20] for a review).

Since the oscillation experiments are continuously making efforts to better determine the oscillation parameters, we find that it is necessary to investigate the Majorana neutrino mass matrix especially after the non-zero and relatively large value of θ_{13} [8, 9]. Regarding an investigation of the neutrino mass matrix after the measurement of θ_{13} , refs. [21] uses inequalities to give the allowed range and the correlations for the absolute values of the neutrino mass matrix elements, and refs. [22] investigates the correlations of the neutrino mass matrix entries by constructing probability distribution functions for each mixing parameters. This paper differs with the other two both in methodology and emphases.

We want to see the constraints on the structure of the Majorana mass matrix given by the current data. Using the simple relation that correlates the mass and the mixing matrix, i.e., $M = U^* \text{diag}(m_1, m_2, m_3) U^\dagger$, we reconstruct the Majorana mass matrix up to an unknown mass. This procedure is taken analytically and the errors of each parameters are carefully passed to the mass matrix entries.

We find that the dominant structure of the Majorana mass matrix at given m_{\min} is still unclear due to the error range of the inputting parameters. But some entries are “grouping” together and different groups are distinguishable at a 3σ level. Furthermore, an approximating μ - τ exchange symmetry is observed in different data sets and different orderings.

This paper is organized as follows. Firstly we reconstruct the Majorana neutrino mass matrix in section 2; Then we discuss the major features of the results and other related issues in section 3; Final conclusion and discussion on the implications for the flavor models come in section 4.

2 Reconstruct the Majorana neutrino mass matrix

2.1 input

The Majorana neutrino mass matrix can be obtained through

$$M = U^* \text{Diag}\{m_1, m_2, m_3\} U^\dagger. \quad (2.1)$$

In the flavor basis, where the charged lepton mass matrix is diagonal, the matrix U diagonalizing the mass matrix M is the PMNS matrix. Since

$$U = VP, \quad P = \text{Diag}\{1, e^{i\frac{\alpha_{21}}{2}}, e^{i\frac{\alpha_{31}}{2}}\}, \quad (2.2)$$

and adopting a standard parametrization [23] for V ,

	best fit	3σ range
$\sin^2 \theta_{12}$	0.306	0.271-0.346
$\sin^2 \theta_{23}$	0.446	0.366-0.663
$\sin^2 \theta_{13}$	0.0231	0.0173-0.0288
$\Delta m_{21}^2 (10^{-5} \text{eV}^2)$	7.45	6.98-8.05
$\Delta m_{31}^2 (10^{-3} \text{eV}^2)$	2.417	2.247-2.623
$\Delta m_{32}^2 (10^{-3} \text{eV}^2)$	-2.411	-2.602- -2.226
$\delta (\text{Degree})$	266	1-360

Table 1. Global fit results from refs. [25].

$$V = \begin{pmatrix} c_{12}c_{13} & s_{12}c_{13} & s_{13}e^{-i\delta} \\ -s_{12}c_{23} - c_{12}s_{23}s_{13}e^{i\delta} & c_{12}c_{23} - s_{12}s_{23}s_{13}e^{i\delta} & s_{23}c_{13} \\ s_{12}s_{23} - c_{12}c_{23}s_{13}e^{i\delta} & -c_{12}s_{23} - s_{12}c_{23}s_{13}e^{i\delta} & c_{23}c_{13} \end{pmatrix}, \quad (2.3)$$

we get the nine parameters in need to determine the Majorana mass matrix

$$\theta_{12}, \theta_{23}, \theta_{13}, \delta, \alpha_{21}, \alpha_{31}, m_1, m_2, m_3.$$

The oscillation experiments measure six of the nine parameters, which are three mixing angles, the Dirac CP-violating phase δ , and two squared mass differences. Though the Dirac CP-violating phase is not determined by the experiments by now, the global fit results give us some clues on its value (see tables 1 and 2). The recent T2K results [24] also suggest a maximal CP-violation with a minus sign, i.e., $\delta = -90^\circ$ (270°), which is in consistent with the global fit.

The Majorana phases contained in the matrix P do not manifest them in the oscillation experiments. Furthermore, we have no knowledge of them. To do the calculation, the two Majorana phases are set to zero by hand. Some comments about this treatment will come in the following section.

Using the whole set of the global fit results [25], together with an assumption of $\alpha_{21} = \alpha_{31} = 0$, we can determine the neutrino mass matrix with an unknown mass standing for the neutrino mass scale. We list the input in table 1. Notice that the octant of θ_{23} is not clear, we use the first octant one just for simplicity. The explicit form of the expressions for $M_{\alpha\beta}$ can be found in section A of the Appendix. Since there is another set of global fit results [26], we use it as an input and list the results in section B of the Appendix.

2.2 extreme case

If the neutrino masses are highly hierarchical, i.e., the lightest neutrino mass is small enough to be neglected, the other two masses can be determined by the two squared mass differences. We consider that a percent level quantity is small enough and make a rough estimate for a to-be-neglected mass scale. Since the small squared mass difference is of $\mathcal{O}(10^{-5})$, the upper limit for the mass-to-be-neglected is the squared root of 10^{-7} , which is of $\mathcal{O}(10^{-4})$.

In the normal hierarchical (NH) case, i.e., $m_1 \leq 10^{-4}$ eV, we omit it and get

$$\begin{aligned} m_2 &\simeq \sqrt{\Delta m_{21}^2} = 0.0086 \text{ eV}; \\ m_3 &\simeq \sqrt{\Delta m_{31}^2} = 0.0492 \text{ eV}; \\ M &\simeq \begin{pmatrix} 0.0015 & 0.0058 & 0.0065 \\ . & 0.0248 & 0.0209 \\ . & . & 0.0292 \end{pmatrix}, \end{aligned} \tag{2.4}$$

where “.” stands for the symmetric counterparts of $|M_{\alpha\beta}|$.

In the inverted hierarchical (IH) case, where $m_3 \leq 10^{-4}$ eV and can be neglected, we have

$$\begin{aligned} m_1 &\simeq m_2 \simeq \sqrt{\Delta m_{32}^2} = 0.0491 \text{ eV}; \\ M &\simeq \begin{pmatrix} 0.0480 & 0.0049 & 0.0055 \\ . & 0.0267 & 0.0250 \\ . & . & 0.0213 \end{pmatrix}. \end{aligned} \tag{2.5}$$

Similarly, if the neutrinos are massive enough to neglect the mass differences, they can be quasi-degenerate (QD). In this case,

$$\begin{aligned} m_1 &\simeq m_2 \simeq m_3 \simeq 0.1 \text{ eV}; \\ M &\simeq \begin{pmatrix} 0.0955 & 0.0200 & 0.0221 \\ . & 0.0980 & 0.0023 \\ . & . & 0.0975 \end{pmatrix}. \end{aligned} \tag{2.6}$$

2.3 general case

We move on to a general case where the unknown lightest neutrino mass is taken to be a variable. We plot the dependence of the $|M_{\alpha\beta}|$ on m_{\min} in figure 1.

According to the stability of the relative magnitudes of different $|M_{\alpha\beta}|$, we recognize three regions with distinct characteristics.

1. For a $m_{\min} < 0.002$ eV, the relative magnitudes of $|M_{\alpha\beta}|$ are stable. We label it as Region I;
2. For $0.002 \text{ eV} < m_{\min} < 0.1 \text{ eV}$, the relative magnitudes change several times (there are several crossings), and the crossing points differ in the normal and the inverted ordering. This region is called Region II;
3. For $m_{\min} > 0.1 \text{ eV}$, the relative magnitudes of $|M_{\alpha\beta}|$ are stable again. It is labeled as Region III.

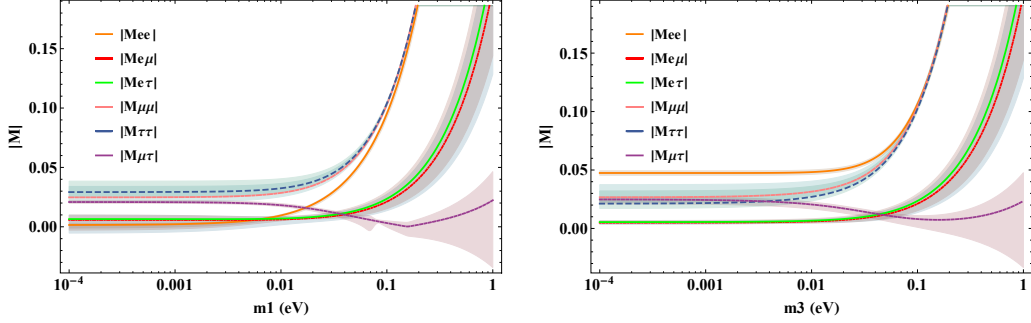


Figure 1. $|M_{\alpha\beta}|$ as a function of the lightest neutrino mass. The left one corresponds to the normal ordering, and the right one corresponds to the inverted ordering. The bands are calculated with the 3σ error ranges of the inputting parameters.

As can be seen from figure 1, this regional division works for both orderings. In Region I and Region III, the stability of the relative magnitudes of $|M_{\alpha\beta}|$ indicates the existence of one dominant structure. The large error ranges in Region III are mainly due to the complex dependence with various inputting parameters.

By far we only use the oscillation data, and it is helpful to get some constraints by using non-oscillation data. We use the combined result from KamLAND-Zen and EXO-200 $\langle m_{\beta\beta} \rangle < (120 - 250) \text{ meV}$ [27], and the Planck 2013 result for $\sum m_\nu < 0.23 \text{ eV}$ [28]. We plot these constraints in figure 2.

We find that the cosmology limit has excluded Region III, while for the constraints from neutrinoless double beta decay experiments, a large part of Region III is excluded. Precision improvements in these experiments will help to narrow the allowed range for the lightest neutrino mass, and distinguish the dominant structure eventually.

3 Discussion

3.1 regional characteristics

In Region I of the normal ordering case, the relative magnitudes determined by the best fit values of the inputting parameters are found to be

$$|M_{\tau\tau}| > |M_{\mu\mu}| > |M_{\mu\tau}| > |M_{e\tau}| > |M_{e\mu}| > |M_{ee}|. \quad (3.1)$$

The first three are of $\mathcal{O}(10^{-2})$, while the latter three are of $\mathcal{O}(10^{-3})$. This means a feature of magnitudes grouping. Different groups are distinguishable in 3σ range. We find $|M_{\mu\mu}| \simeq |M_{\tau\tau}|$ and the curves determined by the best fit values of the inputting parameters lie out of the 3σ range of $|M_{\mu\tau}|$. Similarly, $|M_{e\tau}| \simeq |M_{e\mu}|$ and the curves determined by

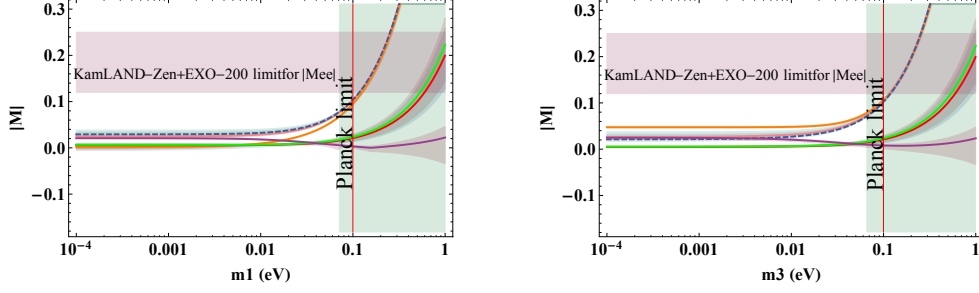


Figure 2. The same as figure 1, with extra demonstration of the exclusion areas setting by the non-oscillation data. The red vertical line distinguishes Region III with Region II, and it is marked in comparison with the Planck limit.

the best fit inputting parameters lie out of the 3σ range of $|M_{ee}|$. Thus the μ - τ exchange symmetry is recognized.

Regarding relations among the mass matrix entries, we make a quick exam about the bimaximal (BM) [29–31] and the tribimaximal (TB) [32, 33] mixing relations, i.e.,

$$M_{ee} = M_{\mu\mu} + M_{\mu\tau}, \quad \text{BM}; \quad (3.2)$$

$$M_{ee} + M_{e\mu} = M_{\mu\mu} + M_{\mu\tau}, \quad \text{TB}. \quad (3.3)$$

Seen from the magnitudes grouping, both of the above relations cannot be satisfied in Region I of the normal ordering. Notice that the TB and the BM mixing also indicate $M_{e\mu} = M_{e\tau}$, $M_{\mu\mu} = M_{\tau\tau}$, which are the relations produced by the μ - τ exchange symmetry and we discuss them separately.

For the inverted ordering in Region I, we have

$$|M_{ee}| > |M_{\mu\mu}| > |M_{\mu\tau}| > |M_{\tau\tau}| > |M_{e\tau}| > |M_{e\mu}|. \quad (3.4)$$

The first four are of $\mathcal{O}(10^{-2})$, while the latter two are of $\mathcal{O}(10^{-3})$. The relations in eqns. 3.2 and 3.3 are satisfied approximately. Combined with the observed μ - τ exchange symmetry, it means the tribimaximal and the bimaximal mixing can be realized in this region.

Figure 3 is offered to see Region II more clearly.

We see that in the normal ordering, the bimaximal relation 3.2 still cannot be satisfied, while the tribimaximal relation 3.3 can be satisfied approximately in $0.05 \text{ eV} < m_1 < 0.08 \text{ eV}$. In the inverted ordering, both of the relations can be satisfied approximately.

Since Region III is excluded by the cosmology limit, we only make a short comment. We also observe the μ - τ exchange symmetry in both orderings. Besides, there are three groups with distinguishable magnitudes, i.e.,

1. $|M_{ee}|, |M_{\mu\mu}|, |M_{\tau\tau}|$, which have the largest magnitudes in given m_{\min} ;

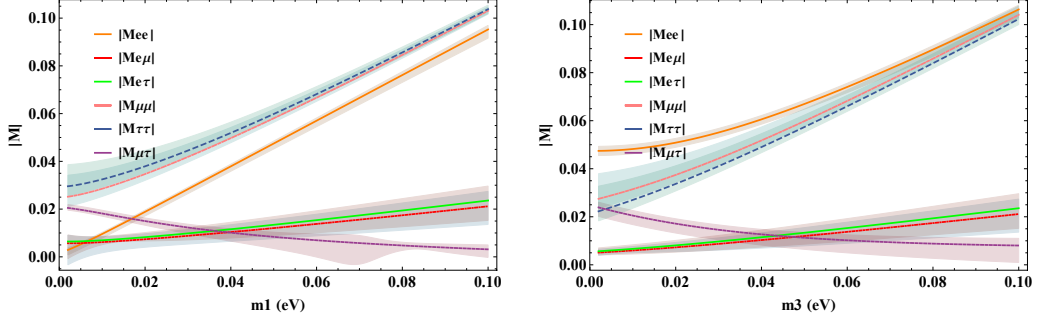


Figure 3. $|M_{\alpha\beta}|$ as a function of the lightest neutrino mass in Region II. The left one corresponds to the normal ordering, and the right one corresponds to the inverted ordering.

2. $|M_{e\mu}|, |M_{e\tau}|$ with an intermediate magnitudes;

3. $|M_{\mu\tau}|$ with the smallest magnitude.

To sum up, we observe an approximating μ - τ exchange symmetry in all the three regions of both the normal and the inverted ordering. We also observe a “grouping effect” in Region I and Region III. Different groups are distinguishable at a 3σ level.

3.2 μ - τ exchange symmetry

As is mentioned, we observe $|M_{e\mu}| \simeq |M_{e\tau}|$, $|M_{\mu\mu}| \simeq |M_{\tau\tau}|$ in all the regions of both orderings. These relations can result from the μ - τ exchange symmetry.

By definition, the μ - τ exchange symmetry is the invariance of the Lagrangian under an exchange of ν_μ with ν_τ . In the Majorana mass term, it means

$$\begin{aligned} \mathcal{L} &= \frac{1}{2}(\bar{\nu}_{eL}, \bar{\nu}_{\mu L}, \bar{\nu}_{\tau L})M(\nu_{eL}^c, \nu_{\mu L}^c, \nu_{\tau L}^c)^T + \text{H.c.} \\ &= \frac{1}{2}(\bar{\nu}_{eL}, \bar{\nu}_{\tau L}, \bar{\nu}_{\mu L})M(\nu_{eL}^c, \nu_{\tau L}^c, \nu_{\mu L}^c)^T + \text{H.c.} \end{aligned} \quad (3.5)$$

Immediately, one arrives at

$$M_{e\mu} = M_{e\tau}, \quad M_{\mu\mu} = M_{\tau\tau}. \quad (3.6)$$

An exchange of ν_μ with ν_τ in the mass term can be performed with the following transformation matrix,

$$A_{23} = \begin{pmatrix} 1 & 0 & 0 \\ 0 & 0 & 1 \\ 0 & 1 & 0 \end{pmatrix}. \quad (3.7)$$

The invariance of the mass term means $A_{23}MA_{23} = M$.

In the flavor basis, the Majorana matrix is diagonalized by the PMNS matrix, i.e., $U^T M U = \text{Diag}\{m_1, m_2, m_3\}$. Thus we get the μ - τ exchange symmetry relation in terms of the mixing matrix entries, i.e.,

$$U_{\mu i} = U_{\tau i}, \quad (3.8)$$

which is necessary and sufficient. Regarding constraints on the mixing angles and the phase, when $|U_{\mu i}| = |U_{\tau i}|$, one gets one of the following two consequences

1. $\theta_{23} = \pi/4, \quad \delta = \pm\pi/2;$
2. $\theta_{23} = \pi/4, \quad \theta_{13} = 0.$

Notice that both of the above two results are necessary but not sufficient condition for the μ - τ exchange symmetry. Notice also the current data indicates a deviation from $\theta_{23} = \pi/4$, which also means the μ - τ exchange symmetry is an approximate symmetry, as can be seen from the figures in this paper directly.

This symmetry has been extensively studied [34–42]. After the measurements of θ_{13} , a dedicated investigation of the μ - τ exchange symmetry can be found in refs. [43]. It is also shown recently that the μ - τ exchange symmetry, in combination with other inputs, can lead to a new mixing pattern which is simple and elegant [44].

3.3 effects of the Majorana phases

To see the effects of the Majorana phases on the structure of neutrino mass, we illustrate the normal ordering results with the Majorana phases $(\alpha_{21}, \alpha_{31})$ setting to pairs of special values in figures 4 and 5. The case of the inverted ordering can be found in section C of the Appendix.

We see that in the cases of non-zero Majorana phases, the general division into three regions according to the stability of the relative magnitudes of different $|M_{\alpha\beta}|$ is applicable. However, the other two major features in the zero-Majorana-phases case, i.e., the magnitudes grouping and the μ - τ symmetry, are changed.

The grouping effect is barely preserved in Region I. In Region III, only the four cases with zero α_{21} exhibit a grouping effect. The μ - τ symmetry is broken in $(\frac{\pi}{2}, 0), (\frac{\pi}{2}, \frac{\pi}{2}), (\frac{\pi}{2}, \frac{3\pi}{2}), (\frac{3\pi}{2}, 0), (\frac{3\pi}{2}, \frac{\pi}{2}), (\frac{3\pi}{2}, \frac{3\pi}{2})$ cases. It is also interesting to note that $|M_{\mu\tau}|$ grows with m_1 more evidently when the Majorana phases are non-zero. Additionally, the error ranges are in general much larger in Region III, due to the complexity increased when the Majorana phases are non-zero.

4 Conclusion

We study the implications for the Majorana neutrino mass matrix given by the current data systematically. The whole set of the oscillation data given by the global fit [25, 26] is used to determine the structure of the Majorana neutrino mass matrix up to the lightest neutrino mass. We make a simple division to the range of m_{\min} by recognizing the differences in

stability of the relative magnitudes of $|M_{\alpha\beta}|$. Then we discuss the regional characteristics. We observe a grouping effect in Region I and Region III and an approximating μ - τ exchange symmetry in all the three regions of both the normal and the inverted orderings. Given m_{\min} , one can read the allowed ranges of $|M_{\alpha\beta}|$ by the current data. Given a mixing pattern, with comparison to our plot, one can find the allowed range of m_{\min} and the information on ordering.

At the m_{\min} range allowed by the current data (both oscillation and non-oscillation), the relative magnitudes of $|M_{\alpha\beta}|$ are not fixed yet. Still, there is information on the dominant structure of the Majorana mass matrix, e.g., different groups of entries are distinguishable at a 3σ level, and a rough structure can be read at a m_{\min} range. We also find that the non-zero Majorana phases change the structural features we mentioned above. It requires precision improvements on these parameters to finally unveil the dominant structure of the Majorana neutrino mass matrix.

These results put extra constraints to the flavor models. A successful model should be able to reproduce the oscillation data. Various models based on special mixing patterns have been proposed initially because the mixing patterns can accommodate the mixing angles approximately. It is reasonable to use the mixing patterns alone as a guidance for building a model that is compatible with the oscillation data. However, a successful model has to do more than that because there are more information provided by the experiments, i.e., the squared mass differences. As can be seen from our discussion about the tribimaximal and bimaximal relations, the mixing patterns can produce a good approximation for the Majorana mass matrix only for some m_{\min} values in certain ordering. It is helpful to point out the regions where the mixing pattern prediction works as an examination to the predictive power of a model.

A The expressions of the entries of the Majorana neutrino mass matrix

$$M_{ee} = c_{13}^2 c_{12}^2 m_1 + c_{13}^2 s_{12}^2 m_2 e^{-i\alpha_{21}} + s_{13}^2 m_3 e^{i(2\delta - \alpha_{31})}; \quad (\text{A.1})$$

$$M_{e\mu} = c_{13}c_{12}(-c_{23}s_{12} - s_{23}c_{12}s_{13}e^{-i\delta})m_1 + c_{13}s_{12}(c_{23}c_{12} - s_{23}s_{12}s_{13}e^{-i\delta})m_2 e^{-i\alpha_{21}} + c_{13}s_{23}s_{13}m_3 e^{i(\delta - \alpha_{31})}; \quad (\text{A.2})$$

$$M_{e\tau} = c_{13}c_{12}(s_{23}s_{12} - c_{23}c_{12}s_{13}e^{-i\delta})m_1 + c_{13}s_{12}(-s_{23}c_{12} - c_{23}s_{12}s_{13}e^{-i\delta})m_2 e^{-i\alpha_{21}} + c_{13}c_{23}s_{13}m_3 e^{i(\delta - \alpha_{31})}; \quad (\text{A.3})$$

$$M_{\mu\mu} = (-c_{23}s_{12} - s_{23}c_{12}s_{13}e^{-i\delta})^2 m_1 + (c_{23}c_{12} - s_{23}s_{12}s_{13}e^{-i\delta})^2 m_2 e^{-i\alpha_{21}} + c_{13}^2 s_{23}^2 m_3 e^{-i\alpha_{31}}; \quad (\text{A.4})$$

$$M_{\mu\tau} = (s_{23}s_{12} - c_{23}c_{12}s_{13}e^{-i\delta})(-c_{23}s_{12} - s_{23}c_{12}s_{13}e^{-i\delta})m_1 + (-s_{23}c_{12} - c_{23}s_{12}s_{13}e^{-i\delta})(c_{23}c_{12} - s_{23}s_{12}s_{13}e^{-i\delta})m_2 e^{-i\alpha_{21}} + c_{13}^2 c_{23}s_{23}m_3 e^{-i\alpha_{31}}; \quad (\text{A.5})$$

$$M_{\tau\tau} = (s_{23}s_{12} - c_{23}c_{12}s_{13}e^{-i\delta})^2 m_1 + (-s_{23}c_{12} - c_{23}s_{12}s_{13}e^{-i\delta})^2 m_2 e^{-i\alpha_{21}} + c_{13}^2 c_{23}^2 m_3 e^{-i\alpha_{31}}. \quad (\text{A.6})$$

	best fit	3σ range
$\sin^2 \theta_{12}$ (N or I)	0.307	0.259-0.359
$\sin^2 \theta_{23}$ (N)	0.386	0.331-0.637
$\sin^2 \theta_{23}$ (I)	0.392	0.335-0.663
$\sin^2 \theta_{13}$ (N)	0.0241	0.0169-0.0313
$\sin^2 \theta_{13}$ (I)	0.0244	0.0171-0.0315
$\delta m^2 (10^{-5} \text{eV}^2)$	7.54	6.99-8.18
$\Delta m^2 (10^{-3} \text{eV}^2)$ (N)	2.43	2.19-2.62
$\Delta m^2 (10^{-3} \text{eV}^2)$ (I)	-2.42	-2.61- -2.17
δ (N)	1.08π	0- 2π
δ (I)	1.09π	0- 2π

Table 2. Global fit results from refs. [26]. N (I) stands for the normal (inverted) ordering.

B The same procedure with Fogli et al. data

We perform the same procedure with the global fit result from refs. [26]. We list the input in table 2, where $\Delta m^2 = m_3^2 - (m_1^2 + m_2^2)/2$. The result is shown in figure 6.

We see that Region I exhibit the same characteristics as the results obtained by using the refs. [25] input, while Region III shows much larger error ranges than in figure 1, which is a result of the mass dependence in Δm^2 definition.

The relative magnitudes are found to be

$$|M_{\tau\tau}| > |M_{\mu\mu}| > |M_{\mu\tau}| > |M_{e\tau}| > |M_{ee}| > |M_{e\mu}| \quad (\text{B.1})$$

in Region I of the normal ordering. The feature of magnitudes grouping is the same as the results we obtained using refs. [25] as an input. The first three are of $\mathcal{O}(10^{-2})$, while the latter three are of $\mathcal{O}(10^{-3})$. $|M_{ee}|$ and $|M_{e\mu}|$ are of different relative magnitudes in comparison with eqn. 3.1.

The relative magnitudes in the inverted ordering case are

$$|M_{ee}| > |M_{\mu\mu}| > |M_{\mu\tau}| > |M_{\tau\tau}| > |M_{e\tau}| > |M_{e\mu}|. \quad (\text{B.2})$$

It is the same as eqn. 3.4.

The μ - τ exchange symmetry is recognized also in all the regions of both the orderings.

C The effects of the Majorana phases in the case of inverted ordering

From figures 7 and 8, we see that the general division into three regions is applicable. The grouping effect is only observed when $\alpha_{21} = 0$ in Region I and $(0, \frac{\pi}{2})$ in Region III. The μ - τ symmetry is broken in $(\frac{\pi}{2}, 0), (\frac{\pi}{2}, \frac{\pi}{2}), (\frac{\pi}{2}, \frac{3\pi}{2}), (\frac{3\pi}{2}, 0), (\frac{3\pi}{2}, \frac{\pi}{2}), (\frac{3\pi}{2}, \frac{3\pi}{2})$ cases. The error ranges are in general large in Region III and $|M_{\mu\tau}|$ grows with m_3 evidently.

Acknowledgments

This work is supported by National Natural Science Foundation of China (Grants No. 11035003 and No. 11120101004).

References

- [1] SNO collaboration, B. Aharmim *et al.*, *Combined Analysis of all Three Phases of Solar Neutrino Data from the Sudbury Neutrino Observatory*, *Phys. Rev. C* **88** (2013) 025501, [arXiv:1109.0763 [nucl-ex]].
- [2] Borexino collaboration, G. Bellini *et al.*, *Final results of Borexino Phase-I on low energy solar neutrino spectroscopy*, arXiv:1308.0443 [hep-ex].
- [3] T2K collaboration, K. Abe *et al.*, *Measurement of the intrinsic electron neutrino component in the T2K neutrino beam with the ND280 detector*, arXiv:1403.2552 [hep-ex].
- [4] OPERA collaboration, N. Agafonova *et al.*, *New results on $\nu_\mu \rightarrow \nu_\tau$ appearance with the OPERA experiment in the CNGS beam*, *JHEP* **1311** (2013) 036, [arXiv:1308.2553 [hep-ex]].
- [5] MINOS collaboration, P. Adamson *et al.*, *Combined analysis of ν_μ disappearance and $\nu_\mu \rightarrow \nu_e$ appearance in MINOS using accelerator and atmospheric neutrinos*, arXiv:1403.0867 [hep-ex].
- [6] NOvA collaboration, M. D. Messier, *Extending the NOvA Physics Program*, arXiv:1308.0106 [hep-ex].
- [7] DOUBLE-CHOOZ collaboration, Y. Abe *et al.*, *Indication for the disappearance of reactor electron antineutrinos in the Double Chooz experiment*, *Phys. Rev. Lett.* **108** (2012) 131801, [arXiv:1112.6353 [hep-ex]].
- [8] DAYA-BAY collaboration, F. P. An *et al.*, *Observation of electron-antineutrino disappearance at Daya Bay*, *Phys. Rev. Lett.* **108** (2012) 171803, [arXiv:1203.1669 [hep-ex]].
- [9] RENO collaboration, J. K. Ahn *et al.*, *Observation of Reactor Electron Antineutrino Disappearance in the RENO Experiment*, *Phys. Rev. Lett.* **108** (2012) 191802, [arXiv:1204.0626 [hep-ex]].
- [10] KamLAND collaboration, A. Gando *et al.*, *Reactor On-Off Antineutrino Measurement with KamLAND*, arXiv:1303.4667 [hep-ex].
- [11] B. Pontecorvo, *Neutrino Experiments and the Problem of Conservation of Leptonic Charge*, *Sov. Phys. JETP* **26** (1968) 984.
- [12] Z. Maki, M. Nakagawa and S. Sakata, *Remarks on the unified model of elementary particles*, *Prog. Theor. Phys.* **28** (1962) 870.
- [13] S. Weinberg, *Baryon and Lepton Nonconserving Processes*, *Phys. Rev. Lett.* **43** (1979) 1566.
- [14] T. Yanagida, *In Proceedings of the Workshop on the Baryon Number of the Universe and Unified Theories*, Tsukuba, Japan, 13-14 Feb 1979.
- [15] P. Minkowski, *$\mu \rightarrow e\gamma$ at a rate of one out of 10^9 muon decays?*, *Phys. Lett. B* **67** (1977) 421.
- [16] S. L. Glashow, *Quarks and Leptons*, in *Cargèse Lectures*, eds. M. Lévy *et al.* Plenum NY, (1980) 687.
- [17] T. P. Cheng and Ling-Fong Li, *Neutrino masses, mixings, and oscillations in $SU(2) \times U(1)$ models of electroweak interactions*, *Phys. Rev. D* **22** (1980) 2860.
- [18] J. Schechter and J. W. F. Valle, *Neutrino masses in $SU(2) \otimes U(1)$ theories*, *Phys. Rev. D* **22** (1980) 2227.
- [19] R. Foot, H. Lew, X. G. He, and G. Joshi, *See-Saw neutrino masses induced by a triplet of leptons*, *Z. Phys. C* **44** (1989) 441.

- [20] G. Altarelli and F. Feruglio, *Discrete Flavor Symmetries and Models of Neutrino Mixing*, *Rev. Mod. Phys.* **82** (2010) 2701, [arXiv:1002.0211 [hep-ph]].
- [21] W. Grimus and P. O. Ludl, *Correlations of the elements of the neutrino mass matrix*, *JHEP* **1212** (2012) 117 [arXiv:1209.2601 [hep-ph]].
- [22] E. Bertuzzo, P. A. N. Machado and R. Z. Funchal, *Neutrino Mass Matrix Textures: A Data-driven Approach*, *JHEP* **1306** (2013) 097 [arXiv:1302.0653 [hep-ph]].
- [23] L. -L. Chau and W. -Y. Keung, *Comments on the Parametrization of the Kobayashi-Maskawa Matrix*, *Phys. Rev. Lett.* **53** (1984) 1802.
- [24] T2K collaboration, K. Abe *et al.*, *Observation of Electron Neutrino Appearance in a Muon Neutrino Beam*, *Phys. Rev. Lett.* **112** (2014) 061802 [arXiv:1311.4750 [hep-ex]].
- [25] M. C. Gonzalez-Garcia, M. Maltoni, J. Salvado and T. Schwetz, *Global fit to three neutrino mixing: critical look at present precision*, *JHEP* **1212** (2012) 123 [arXiv:1209.3023 [hep-ph]].
We use the updated version of results after the 'TAUP 2013' conference from the website <http://www.nu-fit.org>.
- [26] G. L. Fogli, E. Lisi, A. Marrone, D. Montanino, A. Palazzo and A. M. Rotunno, *Global analysis of neutrino masses, mixings and phases: entering the era of leptonic CP violation searches*, *Phys. Rev. D* **86** (2012) 013012 [arXiv:1205.5254 [hep-ph]].
- [27] KamLAND-Zen collaboration, A. Gando *et al.*, *Limit on Neutrinoless $\beta\beta$ Decay of Xe-136 from the First Phase of KamLAND-Zen and Comparison with the Positive Claim in Ge-76*, *Phys. Rev. Lett.* **110** (2013) 6, 062502 [arXiv:1211.3863 [hep-ex]].
- [28] Planck collaboration, P. A. R. Ade *et al.*, *Planck 2013 results. XVI. Cosmological parameters*, arXiv:1303.5076 [astro-ph.CO].
- [29] F. Vissani, *A Study of the scenario with nearly degenerate Majorana neutrinos*, hep-ph/9708483.
- [30] V. D. Barger, S. Pakvasa, T. J. Weiler and K. Whisnant, *Bimaximal mixing of three neutrinos*, *Phys. Lett. B* **437** (1998) 107 [hep-ph/9806387].
- [31] A. J. Baltz, A. S. Goldhaber and M. Goldhaber, *The Solar neutrino puzzle: An Oscillation solution with maximal neutrino mixing*, *Phys. Rev. Lett.* **81** (1998) 5730 [hep-ph/9806540].
- [32] P. F. Harrison and W. G. Scott, *Symmetries and generalizations of tri-bimaximal neutrino mixing*, *Phys. Lett. B* **535** (2002) 163 [hep-ph/0203209].
- [33] P. F. Harrison and W. G. Scott, *Permutation symmetry, tri-bimaximal neutrino mixing and the S_3 group characters*, *Phys. Lett. B* **557** (2003) 76 [hep-ph/0302025].
- [34] T. Fukuyama and H. Nishiura, *Mass matrix of Majorana neutrinos*, hep-ph/9702253.
- [35] R. N. Mohapatra and S. Nussinov, *Bimaximal neutrino mixing and neutrino mass matrix*, *Phys. Rev. D* **60** (1999) 013002 [hep-ph/9809415].
- [36] E. Ma and M. Raidal, *Neutrino mass, muon anomalous magnetic moment, and lepton flavor nonconservation*, *Phys. Rev. Lett.* **87** (2001) 011802 [Erratum-ibid. **87** (2001) 159901] [hep-ph/0102255].
- [37] C. S. Lam, *A 2-3 symmetry in neutrino oscillations*, *Phys. Lett. B* **507** (2001) 214 [hep-ph/0104116].
- [38] W. Grimus and L. Lavoura, *Softly broken lepton numbers and maximal neutrino mixing*, *JHEP* **0107** (2001) 045 [hep-ph/0105212].

- [39] S. Gupta, A. S. Joshipura and K. M. Patel, *Minimal extension of tri-bimaximal mixing and generalized $Z_2 \times Z_2$ symmetries*, *Phys. Rev. D* **85** (2012) 031903 [arXiv:1112.6113 [hep-ph]].
- [40] R. N. Mohapatra and C. C. Nishi, *S_4 Flavored CP Symmetry for Neutrinos*, *Phys. Rev. D* **86** (2012) 073007 [arXiv:1208.2875 [hep-ph]].
- [41] F. Feruglio, C. Hagedorn and R. Ziegler, *Lepton Mixing Parameters from Discrete and CP Symmetries*, *JHEP* **1307** (2013) 027 [arXiv:1211.5560 [hep-ph]].
- [42] M. Holthausen, M. Lindner and M. A. Schmidt, *CP and Discrete Flavour Symmetries*, *JHEP* **1304** (2013) 122 [arXiv:1211.6953 [hep-ph]].
- [43] S. Gupta, A. S. Joshipura and K. M. Patel, *How good is μ - τ symmetry after results on non-zero θ_{13} ?*, *JHEP* **1309** (2013) 035, [arXiv:1301.7130 [hep-ph]].
- [44] H. Qu and B. -Q. Ma, *New mixing pattern for neutrinos*, *Phys. Rev. D* **88** (2013) 037301 [arXiv:1305.4916 [hep-ph]].

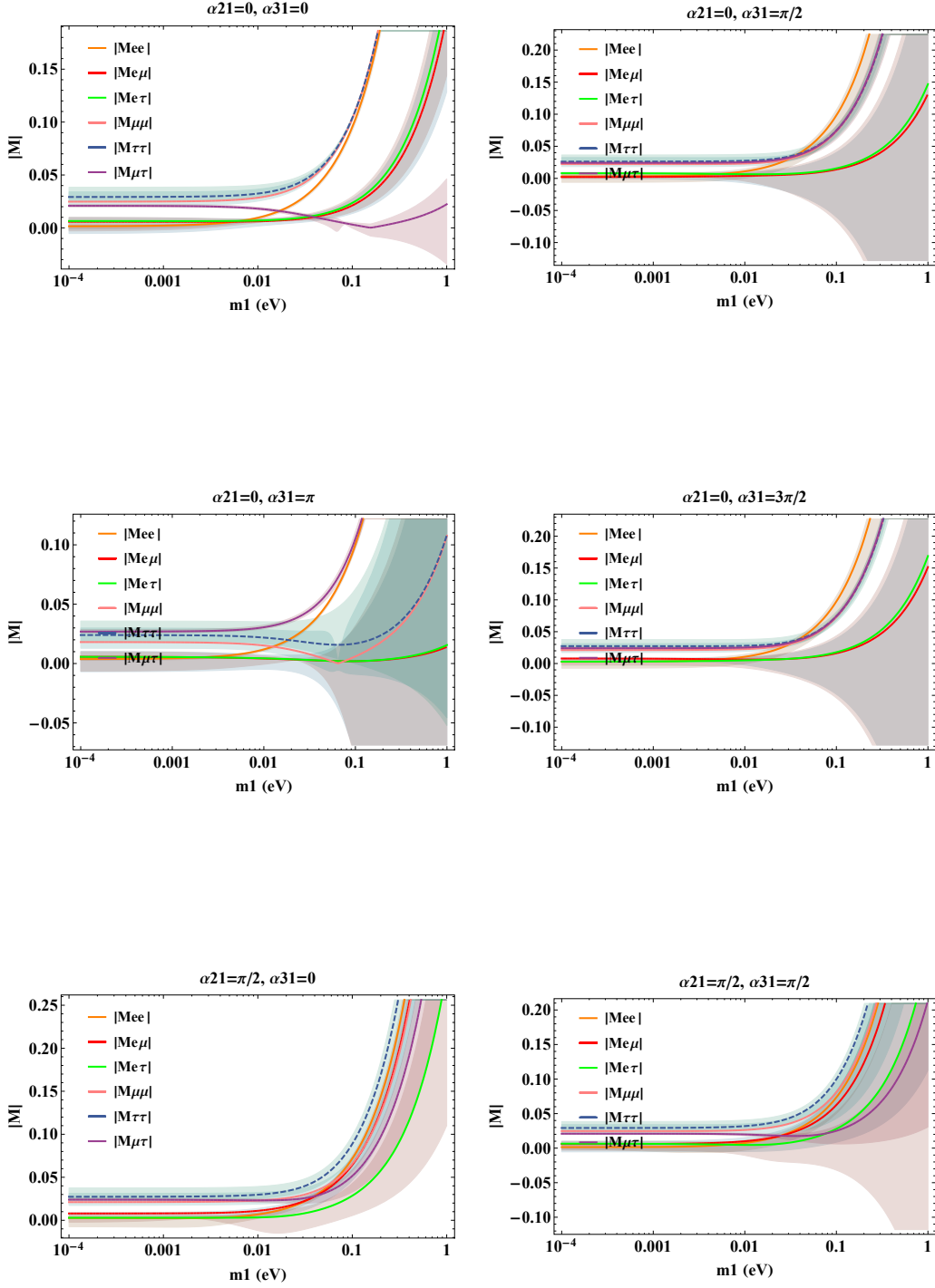


Figure 4. $|M_{\alpha\beta}|$ as a function of the lightest neutrino mass with different pairs of $(\alpha_{21}, \alpha_{31})$ values in the case of the normal ordering.

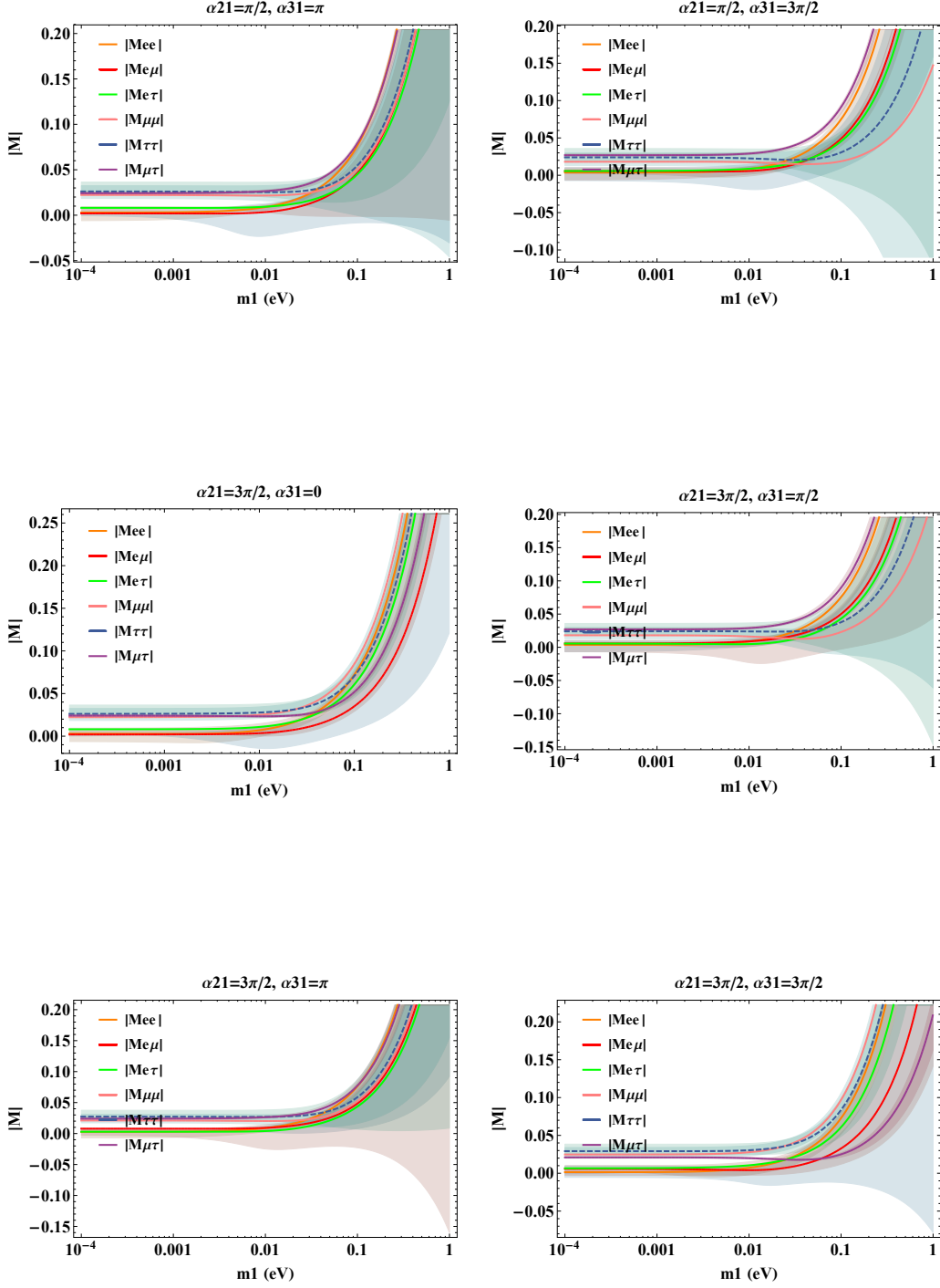


Figure 5. $|M_{\alpha\beta}|$ as a function of the lightest neutrino mass with different pairs of $(\alpha_{21}, \alpha_{31})$ values in the case of the normal ordering.

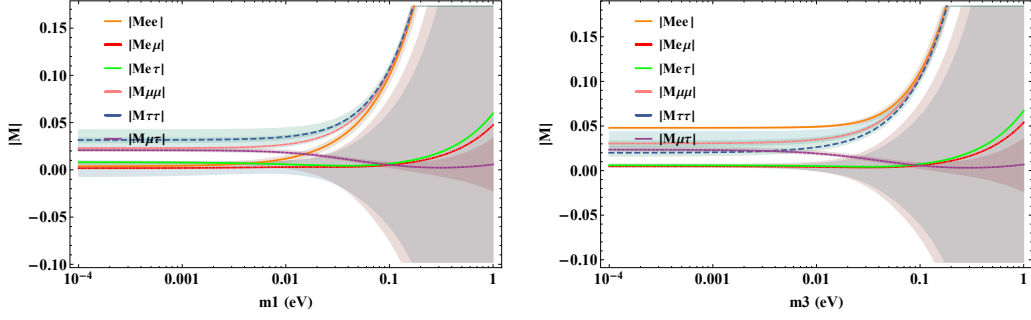


Figure 6. $|M_{\alpha\beta}|$ as a function of the lightest neutrino mass, using refs. [26] as input. The left one corresponds to the normal ordering, while the right one corresponds to the inverted ordering.

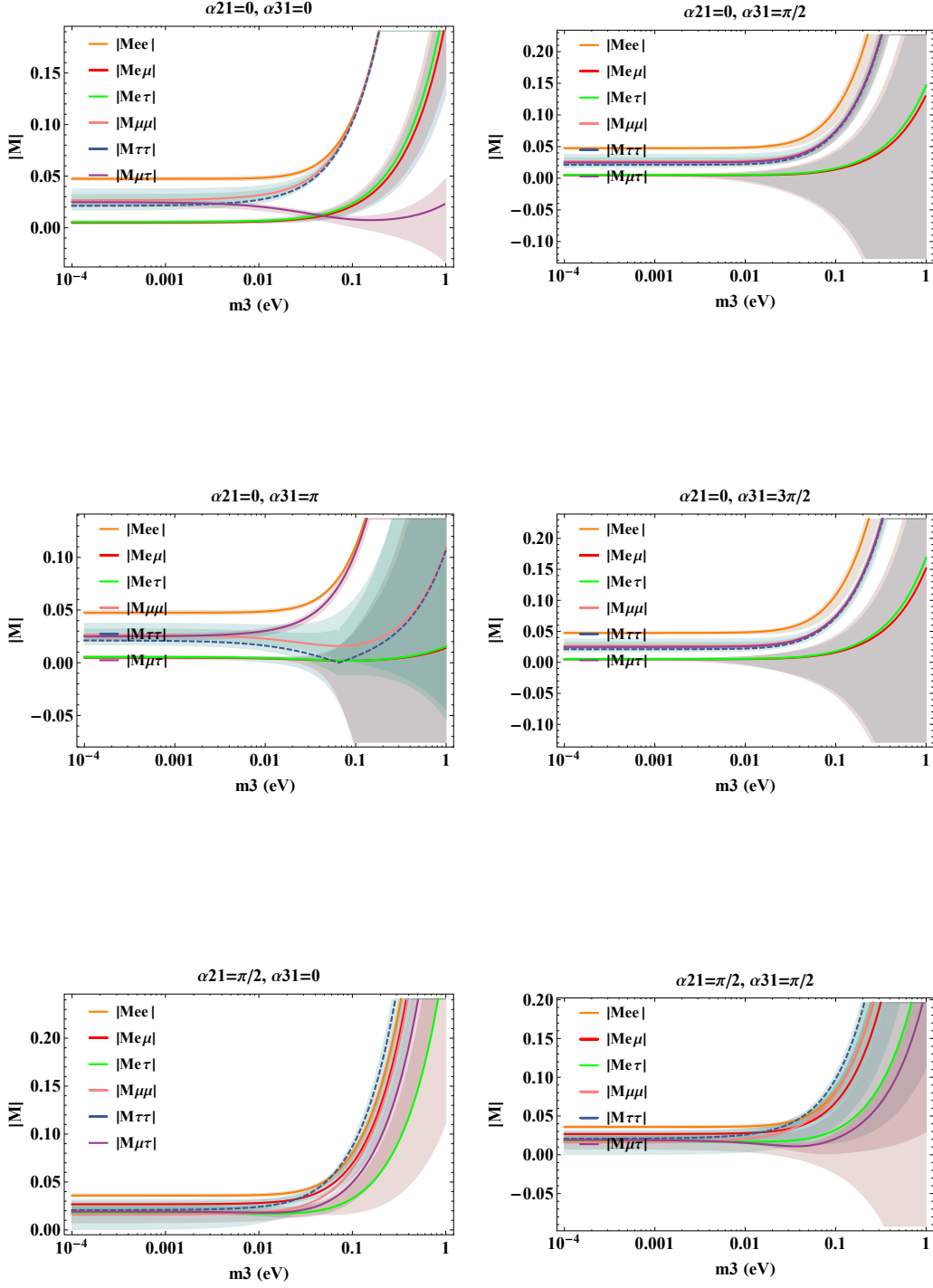


Figure 7. $|M_{\alpha\beta}|$ as a function of the lightest neutrino mass with different pairs of $(\alpha_{21}, \alpha_{31})$ values in the case of the inverted ordering.

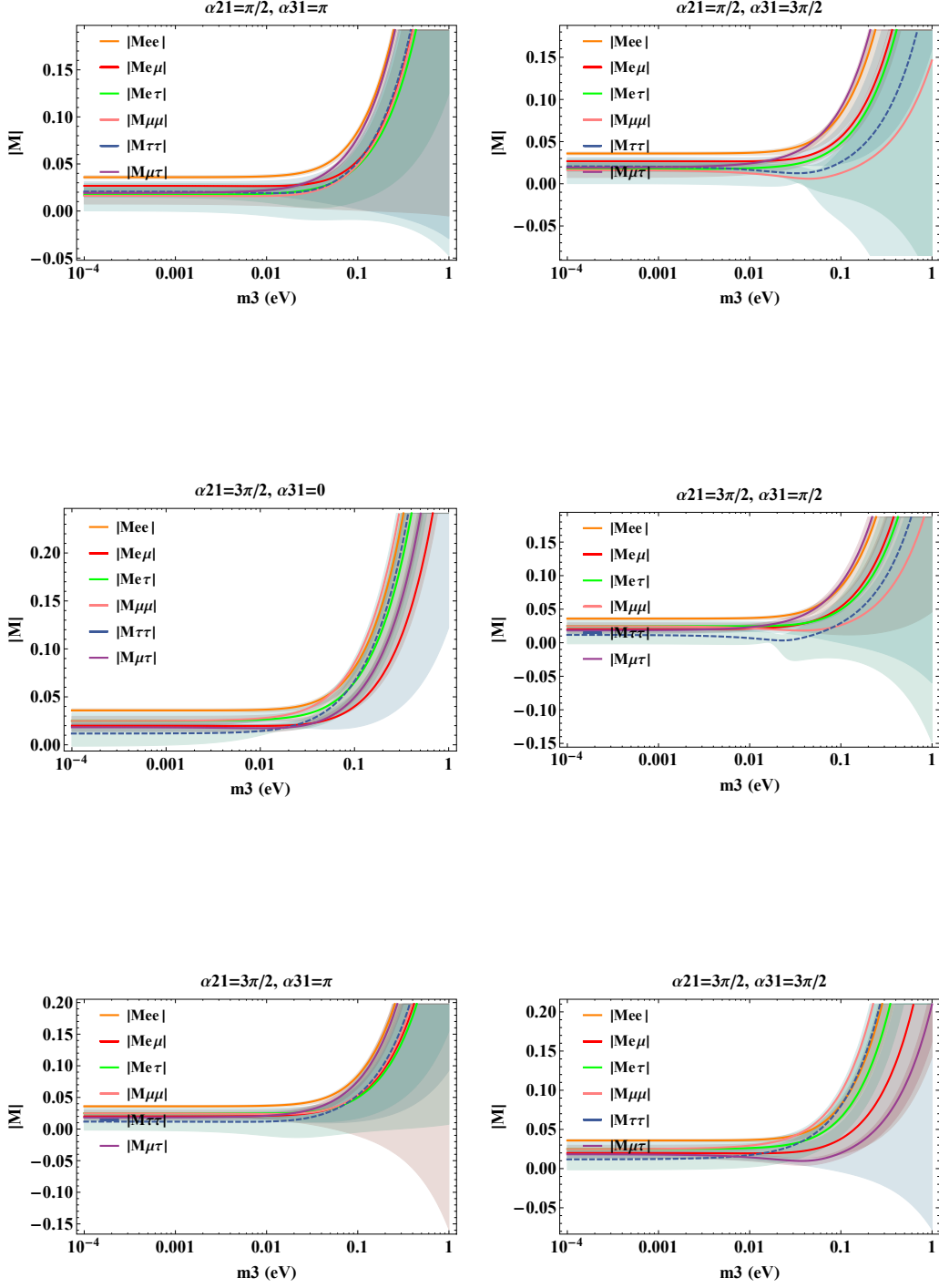


Figure 8. $|M_{\alpha\beta}|$ as a function of the lightest neutrino mass with different pairs of $(\alpha_{21}, \alpha_{31})$ values in the case of the inverted ordering.